JOURNAL OF MATERIALS SCIENCE 30 (1995) 1949–1960

Preparation and properties evaluation of zirconia-based/Al_2O_3 composites as electrolytes for solid oxide fuel cell systems

Part III *Mechanical and electrical characterization*

L. M. NAVARRO, P. RECIO, J. R. JURADO, P. DURAN
Instituto de Ceramica y Vidrio (CSIC), Electroceramics Department, 28500 Arganda del Rey, Madrid, Spain

Yttria-doped zirconia powders containing 3 to 8 mol % Y_2O_3 and 0 to 20 wt % Al_2O_3 were prepared by both mixing commercial oxides and a coprecipitation method, and the mechanical and electrical properties have been examined as a function of the Al_2O_3 content. The bending strength of the composite at room temperature increased with increasing Al_2O_3 content. In the temperature range 500–1000 °C the bending strength increased with Al_2O_3 content up to 10 wt % and then decreased, the measured value at 1000 °C (200 MPa) being higher than those at lower temperatures for cubic zirconia materials. Fracture toughness (K_{IC}) decreased with increasing Y_2O_3 content in the Al_2O_3-free zirconia materials. Al_2O_3 additions enhanced the fracture toughness and this was maximum (7 MPa $m^{1/2}$) for the composite ZrO_2-3 mol % Y_2O_3/ 10 wt % Al_2O_3. The electrical conductivity of cubic ZrO_2/Al_2O_3 composites decreased monotonically with Al_2O_3 content, but in tetragonal ZrO_2/Al_2O_3 composites hardly varied or apparently increased up to 10 wt % Al_2O_3. At 1000 °C the highest electrical conductivity was 0.30 S cm^{-1} for ZrO_2-8 mol % Y_2O_3, and this decreased up to 0.10 S cm^{-1} for the composite ZrO_2-8 mol % Y_2O_3/20 wt % Al_2O_3.

1. Introduction

This is the last part of a series of papers on understanding the influence of Al_2O_3 additions on the particle size and morphology of zirconia powders. Part 1 [1], and Part 2 [2] presented the densification behaviour and the developed microstructures in the above-mentioned compacted powders. It was concluded (a) that the presence of Al_2O_3 increased the specific surface of the coprecipitated zirconia powders; (b) the zirconia crystallization was retarded as a consequence of a polycondensation reaction in which the intercalation of –O–Al–O– groups increased the Zr–Y interdiffusion distances; (c) alumina additions (up to 10 wt %) enhanced the densification of zirconia powders; and (d) the grain growth process of the zirconia grains was strongly hindered by the presence of Al_2O_3 inclusions in the zirconia matrix.

In developing a solid oxide fuel cell (SOFC), the planar configuration seems to be the most promising as against the other two tubular and monolithic configurations for electric power generation systems [3–5]. This type of SOFC is being developed in Europe and Japan, and the two main problems, among others, in developing a high performance planar cell are related to the ionic conductivity and the mechanical properties of the electrolyte. The contribution of the electrolyte resistance to the total cell resistance is so high that the electrical conductivity of the electrolyte determines in great measure the cell performance.

Since fully stabilized zirconia (FSZ) offers a higher ionic conductivity [6, 7], FSZ has been applied to SOFC as electrolyte. However, FSZ, although stable over a wide temperature range, is extremely brittle. On the other hand, partially stabilized zirconia (PSZ), having a lower yttria dopant concentration, consists mainly of the tetragonal phase and possesses greater strength and toughness, as a consequence of the stress-induced tetragonal to monoclinic transformation. But this phenomenon can cause an ageing problem in this tough material and its electrical conductivity at the operating temperature of the SOFC is one order of magnitude lower than that of FSZ at 1000 °C [8].

Many efforts have been and are being carried out to improve both the mechanical properties of FSZ and the PSZ ageing degradation. Thus Al_2O_3, having an elastic modulus twice that of ZrO_2, has been considered as a suitable additive to retain the tetragonal phase in the Al_2O_3/ZrO_2 composite [9], and Tsukuma *et al.* [10] reported that the addition of Al_2O_3 enhanced the room temperature strength and fracture toughness of Y-TZP. In the same way it was also reported [10–12] that the low-temperature tetragonal to monoclinic transformation could be retarded by the addition of Al_2O_3 to Y-TZP.

0022–2461

Since Butler and Drennan's [13] suggestion of the scavenger effect of Al_2O_3 for SiO_2 resulting in a reduced zirconia resistivity, many papers have been devoted to the study of the effect of Al_2O_3 additions on the electrical properties of zirconia-based ceramics. Thus, Bernard [14] reported that Al_2O_3 additions lowered the overall and grain-boundary resistivity of fully stabilized zirconia (FSZ), and Butler *et al.* [15] also reported the beneficial effects of small Al_2O_3 additions on the total conductivity of these materials. In contrast, Inozemtsev and Perfilev [16] and Verkerk *et al.* [17] found that Al_2O_3 additions increase both the bulk and grain-boundary resistivity of FSZ. Badwal *et al.* [18] and Rajendran *et al.* [19] reported that large additions of Al_2O_3 (5–50 wt %) have a negative effect on the conductivity of fully stabilized zirconias.

The present work was devoted to the study of the effect of Al_2O_3 additions (5–20 wt %) on both the mechanical and the electrical properties of a series of yttria-doped ZrO_2-based materials.

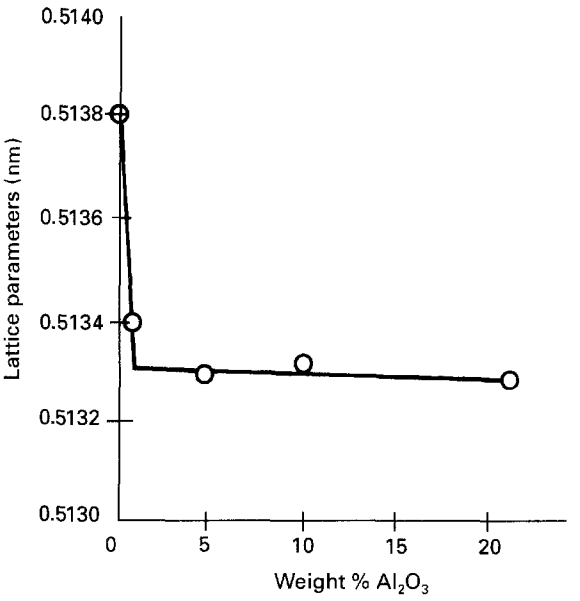

Figure 1 Lattice parameters of cubic stabilized zirconia (Z-8Y) as a function of Al_2O_3 content.

2. Experimental procedure

The two kinds of zirconia powders (commercial and coprecipitated), prepared as described elsewhere [1], were isostatically pressed at 200 MPa and sintered at the temperature interval of 1400 to 1600 °C for 2 h. Only those zirconia samples having high density and good microstructure were chosen for characterization. The bulk density of the sintered samples was measured by the Archimedes displacement method with water.

X-ray diffraction of sintered samples was obtained using a Siemens 5000D model diffractometer with monochromated CuKα radiation and a scintillation detector. In all cases silicon powder was used as an internal standard, and lattice parameters were calculated with a precision of $\pm$ 0.0005 nm.

Hardness (H) and fracture toughness (K_{IC}) experiments were performed on surfaces polished to 1 μm diamond finish using a Vickers pyramid indenter at a load of 10N. H and K_{IC} calculations were made using the formula proposed by Anstis *et al.* [20].

The samples were cut into bars of $30 \times 5 \times 2$ to measure bending strength. After polishing, strength measurements were carried out using a four-point test fixture with an inner span of 20 mm and an outer span of 40 mm. The dependence of bending strength on temperature was measured at room temperature and at 1000 °C. All the samples were equilibrated for 0.5 to 1 h at the fixed temperature before measuring, and 3 to 5 samples were measured for each data point using the standard formula $\sigma_f = 3PL/bw^2$.

Additional three-point bending measurements were also carried out on cylindrical samples 80 mm long and 5 mm in diameter in a universal test Instron machine with a span of 10 mm. The measurements were carried out in the temperature range 25–1000 °C.

The electrical conductivity measurements were carried out on sintered discs about 1 cm in diameter and about 0.2 cm thick with platinum paint electrodes sintered at 800 °C for 0.5 h. The a.c. conductivity was measured using a frequency-response analyser (H.P. 4192 A) over a frequency range of 10 Hz to 10×10^6 Hz with an applied potential of 0.5 V and in the temperature range 200–1000 °C in air.

SEM photographs of the external and fracture surfaces were taken using a Carl Zeiss 500 E, and grain sizes were measured by the line interception method [21].

3. Experimental results

3.1. X-ray diffraction and EDX studies

The XRD results obtained in the compositions studied corresponded well with the phases distribution established in the ZrO_2–Y_2O_3 system [22]. Thus the X-ray patterns of Z-3Y sintered samples showed the only tetragonal zirconia phase. A mixture of the predominant tetragonal zirconia and a small amount of cubic phase was present in the Z-4Y compositions. In the Z-6Y composition also, a mixture of tetragonal zirconia (small amount) and a predominant cubic zirconia phase was found. Finally, a clear cubic phase of fully stabilized zirconia was present in the Z-8Y compositions.

Lattice parameters of the cubic zirconia solid solutions decreased with additions of Al_2O_3 as shown in Fig. 1 and that means that some of the Al^{3+} ions substituted for Zr^{4+} ones in the zirconia structure. The lattice parameter of the Z-8Y sample is 0.51381 nm which is in good agreement with reported values for FSZ (8 mol % Y_2O_3) [23]. The lattice parameter of Z-8Y decreases up to a value of 0.51340 nm and then remains constant. This lattice parameter value establishes the solubility limit of Al_2O_3 in ZrO_2 in 0.7 mol % at 1650 °C.

The above results were corroborated by the EDX analysis carried out on a Z-8Y/20A sample sintered at 1650 °C. Fig. 2a and b shows the EDX spectra of the phases present in the Al_2O_3 particles and in the zirconia grains. EDX analysis indicates that the Al_2O_3 particles contained mainly Al and small quantities of

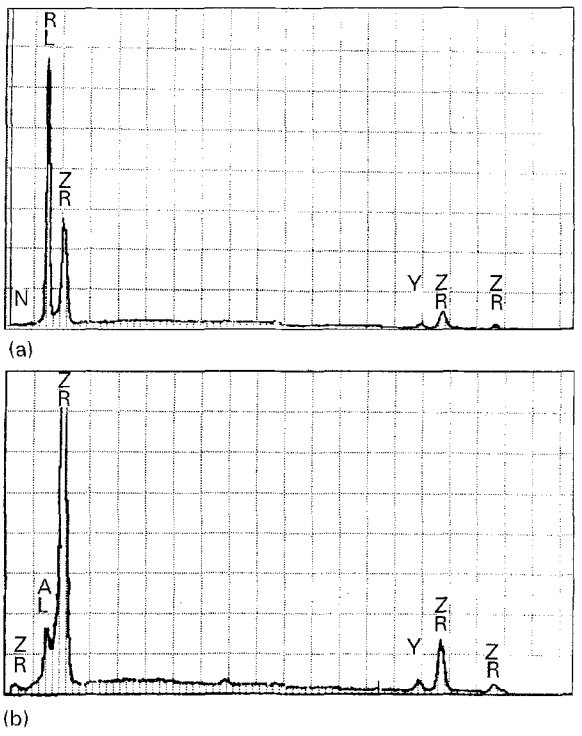

Figure 2 EDX analysis of (a) alumina particles and (b) cubic zirconia grains in a Z-8Y/20A sample.

Zr and Y. The average composition of Al_2O_3 particles was 90.2 wt % Al_2O_3, 8.1 wt % ZrO_2, and 1.7 wt % Y_2O_3. This result is not in agreement with the Al_2O_3–ZrO_2–Y_2O_3 [24] ternary system, but it indicates that some amount of ZrO_2 and Y_2O_3 forms a solid solution or compound with Al_2O_3. In the same way the ZrO_2 grains had an average composition of 83.5 wt % ZrO_2, 4.19 wt % Al_2O_3 and 12.30 wt % Y_2O_3. Because of the large errors usually involved in EDX analysis, it is very difficult to establish with precision the concentration of the oxides entering in solid solution into both the ZrO_2 grains and the Al_2O_3 particles. However, an Al enrichment of the ZrO_2 grains and a Zr and Y enrichment of the Al_2O_3 particles could be assumed. In both cases a chemical formula $(ZrO_2)_a(Al_2O_3)_b(Y_2O_3)_c$ in which $a + b + c = 1$ must be maintained, given that no other oxides were detected.

3.2. Mechanical properties

The bulk densities and mechanical properties of the chosen commercial and coprecipitated zirconia/Al_2O_3 composites are given in Table I. As shown in the table, the effects of powder preparation on hardness (H) are insignificant. The fracture toughness (K_{IC}) was strongly influenced by the microstructure of the sintered samples. Thus the highest K_{IC} value was achieved for the case of the Z-3Y/10A coprecipitated sample (7 $MPam^{1/2}$) as a consequence of a more homogeneous microstructure and a smaller grain size (0.2 μm). Fig. 3a and b shows the indentation behaviour for a commercial sample and a coprecipitated sample, respectively, while Fig. 3c and d shows a crack deflection toughening mechanism. In the same way the deflection toughening mechanism was also present in the coprecipitated zirconia/Al_2O_3 composites as shown in Fig. 4a and b.

The three-point bending strength as a function of the alumina content for the commercial zirconia Z-8Y samples sintered at 1650 °C is given in Fig. 5 for several temperatures. As can be seen, the bending strength showed a maximum at 10 wt % Al_2O_3 in all cases. It can also be seen that the bending strength decreased from room temperature up to 500 °C and then increased at higher temperatures. Fig. 6 shows the fresh fracture surface of the Z-8Y sintered samples containing 0 to 20 wt % Al_2O_3 in which a transition from transgranular to intergranular mode was present.

The four-point bending strength was measured as a function of the Y_2O_3 content for those zirconia samples containing 0 and 10 wt % Al_2O_3 at room temperature and at 1000 °C, as shown in Fig. 7. It can be observed that the bending strength decreased as the Y_2O_3 content increased, and this trend is similar for the compositions containing 10 wt % Al_2O_3. It must be mentioned that the Al_2O_3 addition enhanced the bending strength not only at room temperature but also at 1000 °C. Fig. 8 shows the effect of processing defects such as voids and/or agglomerates as fracture origins leading to a lowering of the mechanical properties.

3.2. Electrical properties

The electrical measurements were carried out on the above-mentioned zirconia compositions sintered at

TABLE I Density, hardness and fracture toughness of sintered zirconia/Al_2O_3 composites

Samples	Commercial			Coprecipitated		
	% TD	H(GPa)	K_{IC} (MPa $m^{1/2}$)	% TD	H(Gpa)	K_{IC} (MPa $m^{1/2}$)
Z3Y	98.0	13.5	5.2	99	12.8	5.5
Z-3Y/10A	97.0	13.3	5.7	97	13.0	7.0
Z-4Y	96.0	13.6	3.9	96	12.1	3.8
Z-4Y/10A	97.0	12.8	4.5	97	13.5	5.5
Z-6Y	95.0	12.8	2.5	96	11.0	3.2
Z-6Y/10A	98.0	13.7	4.0	98	13.5	4.2
Z-8Y	98.0	13.0	2.0	95	13.0	2.1
Z-8Y/5A	97.0	12.9	2.1			
Z-8Y/10A	97.0	14.0	2.4	99	13.0	3.0
Z-8Y/20A	85.0	14.0	2.4			

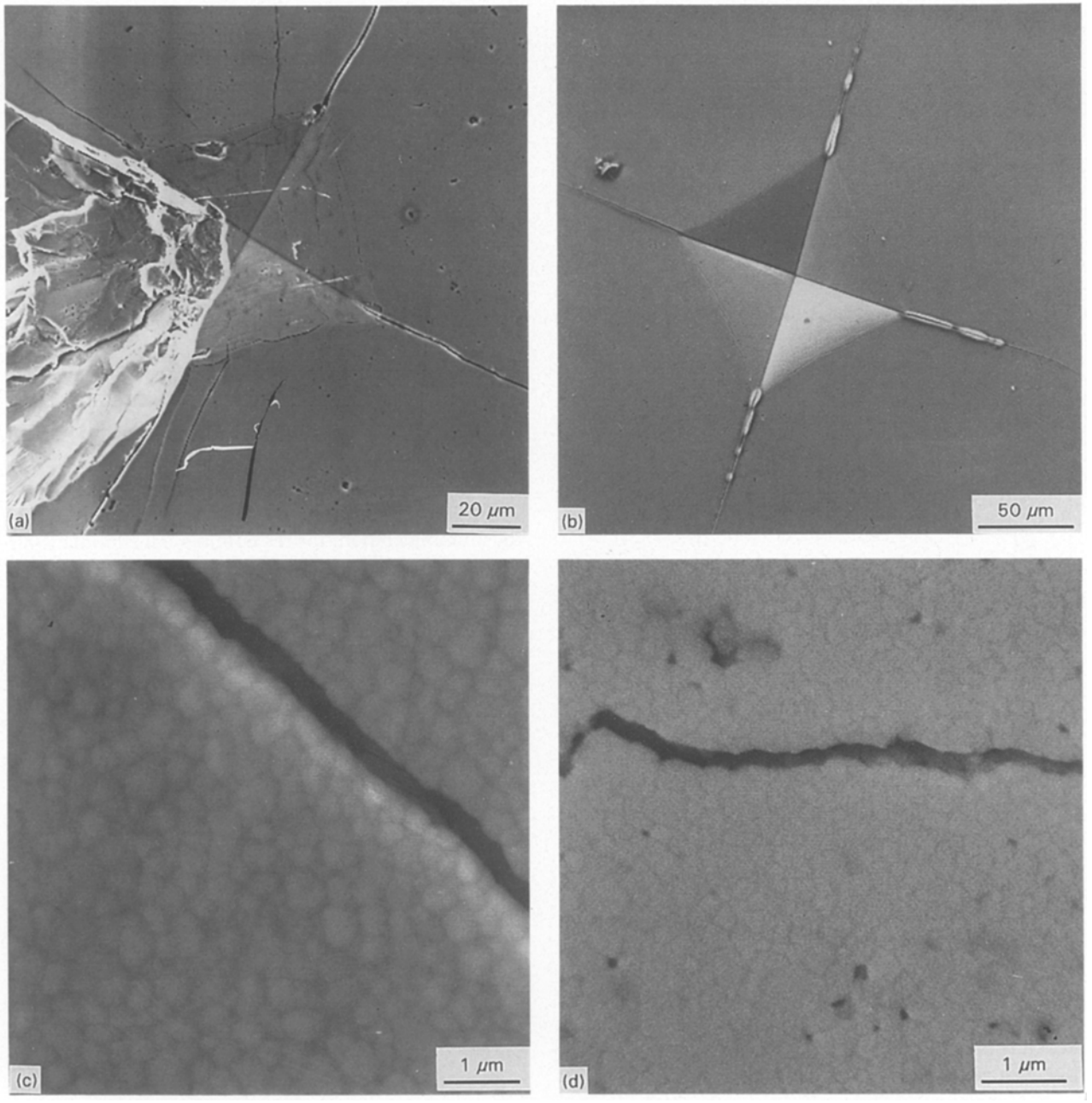

Figure 3 Indentation behaviour of a Z-3Y commercial sample (a), coprecipitated (b), and the deflection toughening mechanism present in both samples (c) and (d), respectively.

1400 °C for which the densification level of the samples was higher than 95% theoretical density and, therefore, the effect of porosity on the conductivity can be considered as negligible. Thus Fig. 9 shows the variation of the total conductivity σ_T of commercial zirconia samples as a function of the Al_2O_3 content. As can be seen, Al_2O_3 additions led to a decrease in conductivity in all the cases of the zirconia commercial samples, and such a decrease was more significant for Z-8Y samples. In spite of this, the difference between the alumina-free sample and that containing 20 wt % Al_2O_3 was not too high; $0.30\,\Omega^{-1}\,cm^{-1}$ and $0.10\,\Omega^{-1}\,cm^{-1}$ at 1000 °C respectively.

Figs 10 and 11 show the influence of both the Al_2O_3 additions and sintering temperature on the resistivity of commercial tetragonal zirconia samples and cubic zirconia ones, respectively. The resistivity of zirconia samples increased monotonically with Al_2O_3 content, and such an influence was clearer at the higher sintering temperature.

Fig. 12 shows the effect of the 10 wt % Al_2O_3 addition on the a.c. conductivity at 300 °C of commercial zirconia samples with different Y_2O_3 content, and a displacement of the grain-boundary arc to the left of the spectrum, indicating a lower total resistivity, can be observed. It must be mentioned that the average grain size of the sintered samples was 0.30 μm, 2.0 μm, 4.0 μm and 4.3 μm for Z-3Y/10A, Z-4Y/10A, Z-6Y/10A and Z-8Y/10A samples, respectively, as measured from the microstructures shown in Fig. 13.

The total conductivity of Z-8Y and Z-8Y/10A samples as a function of temperature is plotted in Fig. 14. The same trends were found in the Arrhenius plots for the other zirconia samples containing Al_2O_3. The activation energy values were very similar, being 1.17, 1.19, 1.16 and 1.13 eV for the Z-8Y, Z-8Y/5A,

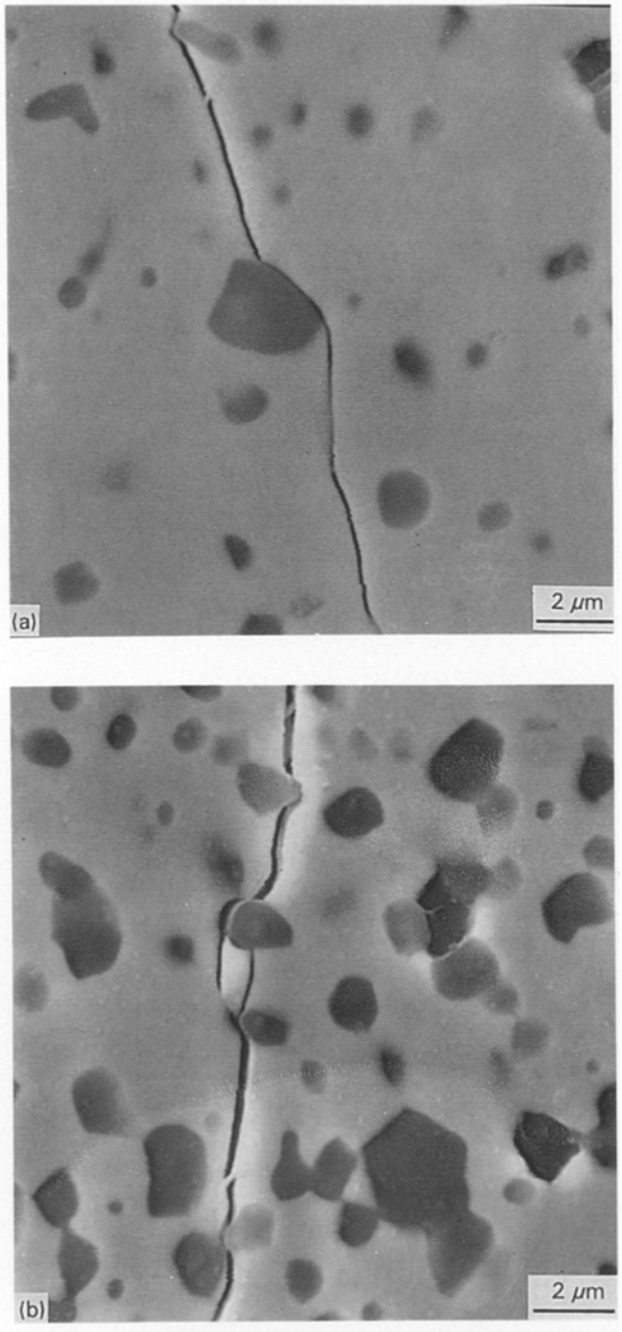

Figure 4 SEM photographs showing a crack deflection toughening mechanism in (a) Z-8Y/5A and (b) Z-8Y/20A composites.

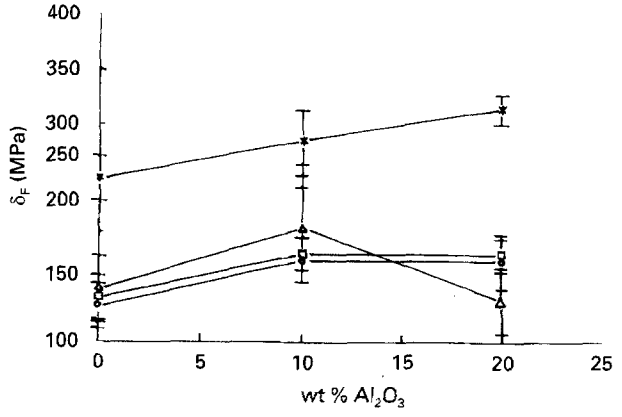

Figure 5 Effect of Al_2O_3 content on three-point bending strength at several temperatures. Sintering temperature 1650 °C. *—*—*—* at 25 °C; O—O—O—O at 500 °C; □—□—□—□ at 800 °C; △—△—△—△ at 1000 °C.

Z-8Y/10A and Z-8Y/20A samples, respectively. However, it must be noted that in the case of the Z-3Y zirconia samples with or without Al_2O_3, having a tetragonal structure, the activation energy values were somewhat lower than those of the cubic stabilized zirconia samples. Thus the activation energy for the Z-3Y sample was 0.92 eV and that of the Z-3Y/20A sample 0.91 eV.

Fig. 15 shows the impedance spectra for the zirconia coprecipitated samples containing 0 and 10 wt % Al_2O_3. Generally it can be said that the conductivity of the alumina-free coprecipitated zirconia samples was slightly higher than those of the corresponding commercial zirconia ones. This can be explained by a more uniform microstructure and a higher densification. However, from the same figure it can be observed that the addition of 10 wt % Al_2O_3 strongly increased the grain boundary contribution to the total resistivity of the sample and thus decreased its total conductivity. A comparison of the typical microstructures is shown in Fig. 16 for the commercial and coprecipitated Z-4Y and Z-6Y zirconia samples containing 10 wt % Al_2O_3.

Fig. 17 displays the Arrhenius plot for the Z-8Y and Z-8Y/10A coprecipitated zirconia samples in which the detrimental influence of the Al_2O_3 addition on conductivity can be observed, mainly, at medium and low temperatures. The activation energy values trend was similar to that present in the commercial zirconia samples.

4. Discussion

The above-described experimental results on the mechanical and electrical properties of several yttria-doped zirconia/Al_2O_3 composites could be explained as follows.

From the X-ray results it is suggested that Al_2O_3 additions to yttria-doped zirconia could interact in three different ways: (a) some of the Al_2O_3 (about 0.7 mol %) goes into the zirconia matrix forming a solid solution; (b) the Al_2O_3 remaining, if the chemical potential of Y_2O_3 in an Al_2O_3–Y_2O_3 compound (for example $Y_6Al_{10}O_{24}$, $AlYO_3$ or $Y_2Al_2O_3$) is lower than in the zirconia matrix, then some of Y_2O_3 will react with Al_2O_3 forming a solid solution, if any, or an Al_2O_3–Y_2O_3 compound; (c) if the above condition is not satisfied then the Al_2O_3 remaining, depending on the sintering temperature, will locate within or between zirconia grains. The decrease of the zirconia lattice parameters (see Fig. 1), and the appearance of some amount of Y_2O_3 in the Al_2O_3 particles (see Fig. 2) evinced a certain reaction between Al_2O_3 and yttria-stabilized zirconia. The possibility of the formation of an Al_2O_3–Y_2O_3 compound, although it could not be detected by XRD, should be taken into account. Thermodynamic and kinetic considerations support such an idea.

Concerning the mechanical properties of tetragonal zirconia/Al_2O_3 composites, it was well established that the stress-induced martensitic phase transformation is the toughening agent. According to our results (see Table I), density and grain size had a strong

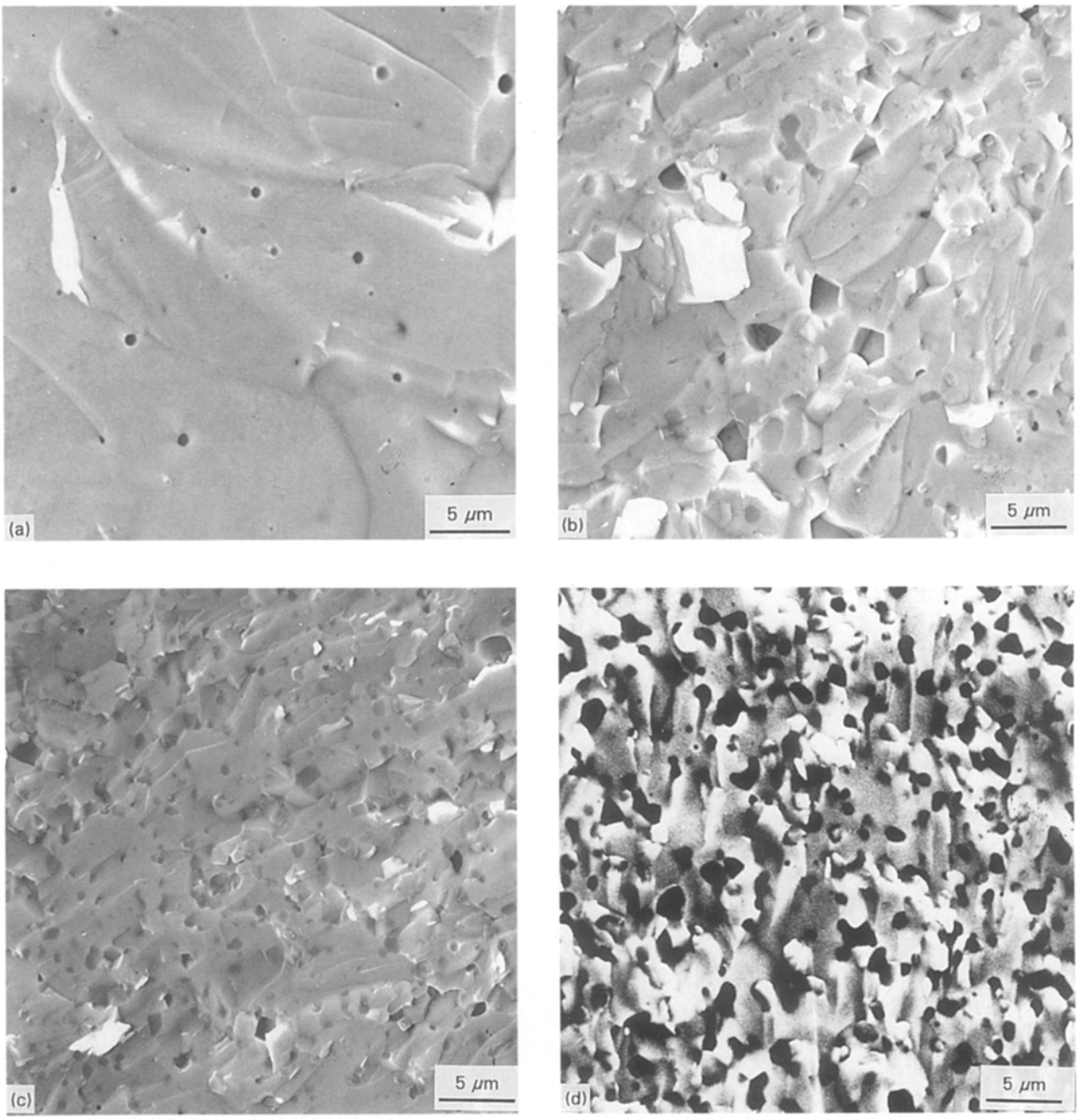

Figure 6 Evolution of fracture surface of Z-8Y sample as a function of the Al_2O_3 content, (a) 0 wt % Al_2O_3, (b) 5 wt % Al_2O_3, (c) 10 wt % Al_2O_3, and (d) 20 wt % Al_2O_3.

influence on the fracture toughness of Z-3Y compositions and a relative influence on the hardness. As shown in the table, the fracture toughness at room temperature was higher in the coarse-grained samples without Al_2O_3. However, in the tetragonal zirconia/Al_2O_3 composites the fracture toughness was higher in those samples having a smaller grain size. Thus commercial Z-3Y/10A with an average size of 0.30 μm had a K_{IC} of $\sim 5.7\ MPam^{1/2}$, and the co-precipitated Z-3Y/10A with a grain size of 0.20 μm presented a K_{IC} of $7\ MPam^{1/2}$. This being so, the participation of another toughening mechanism as the crack deflection one (See Fig. 4) should be taken into account. In the case of the Z-4Y and Z-6Y samples with or without Al_2O_3, the fracture toughness is lower (3.9 to 5.5 $MPam^{1/2}$) due to the increased Y_2O_3 content. In both cases, hardness and fracture toughness were improved by the Al_2O_3 additions. Generally, and according to the XRD results, the increase in the cubic zirconia phase implied a decrease in the tetragonal one which, on the other hand, could justify the decrease of K_{IC} as Y_2O_3 increased.

At room temperature, the three-point bending strength in all the cubic zirconia samples increased with increasing Al_2O_3 (see Fig. 5); this is a consequence of both the higher bending strength of the Al_2O_3 particles and the generated strains in view of the different expansion coefficients of the two components. These results conflict with those reported by Kulczycki and Wasincionek [25] but are in close agreement with those of Esper *et al.* [26] and Yamamoto *et al.* [27]. Kulczycki and Wasincioneck

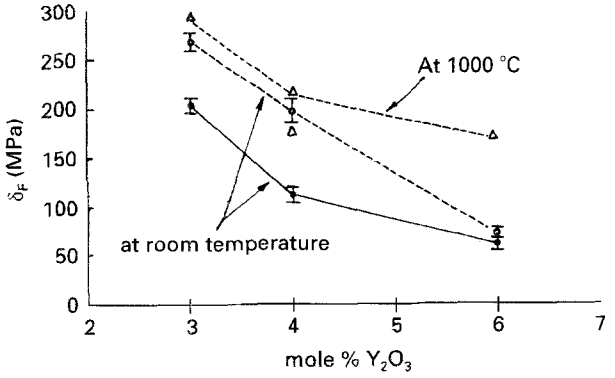

Figure 7 Effect of Y_2O_3 content on the four-point bending strength of Z-8Y and Z-8Y/10A samples at room temperature and at 1000 °C. ●—●—● 0 wt % Al_2O_3; △—△—△ and ○–○–○ 10 wt %.

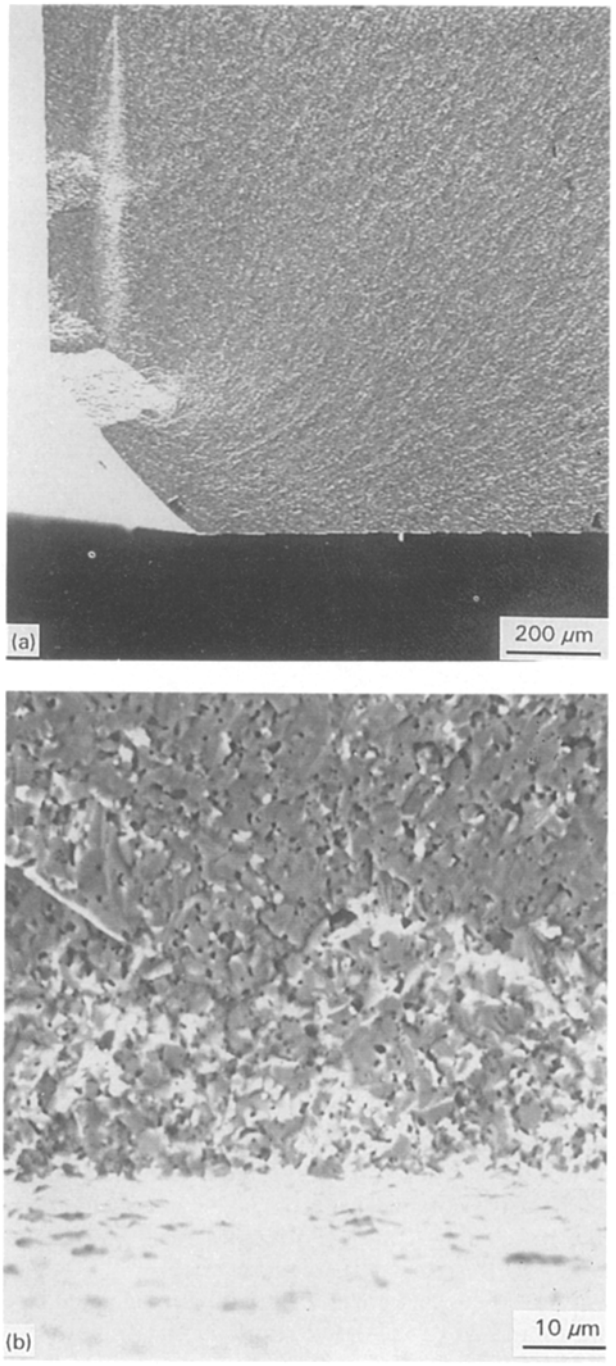

Figure 8 Effect of defects processing (a) laminations and (b) agglomerate on the mechanical behaviour of a Z-6Y/10A composite.

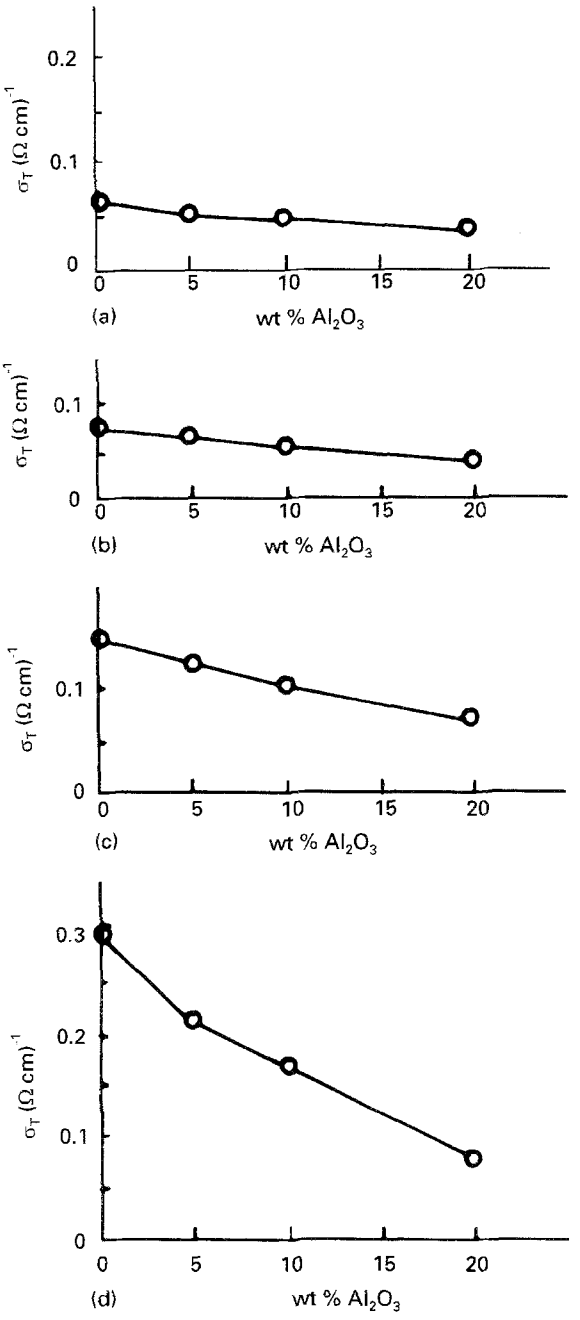

Figure 9 Effect of Al_2O_3 content on the total conductivity σ_T of different yttria-doped zirconia samples. (a) Z-3Y; (b) Z-4Y; (c) Z-6Y; (d) Z-8Y.

[25] reported that the bending strength of ZrO_2-6.5 mol % Y_2O_3 decreased with Al_2O_3 additions up to 20 wt %, and then increased for higher Al_2O_3 content. However, Esper *et al.* [26] and Yamamoto *et al.* [27] found that the fracture strength of fully stabilized zirconia improved with the addition of Al_2O_3 and a maximum was present at 20 wt % Al_2O_3. Rajendran *et al.* [28] found an enhancement of the modulus of rupture of Y-TZP materials by the Al_2O_3 additions, the maximum being for the 20 wt %.

At high temperature the three-point bending of Z-8Y commercial samples increased as the Al_2O_3 content increased up to 10 wt % and then decreased. It must be noted that the bending strength was higher at 1000 °C than at 500 °C, and it was near to that of room temperature (see Fig. 5). Although only the addition of

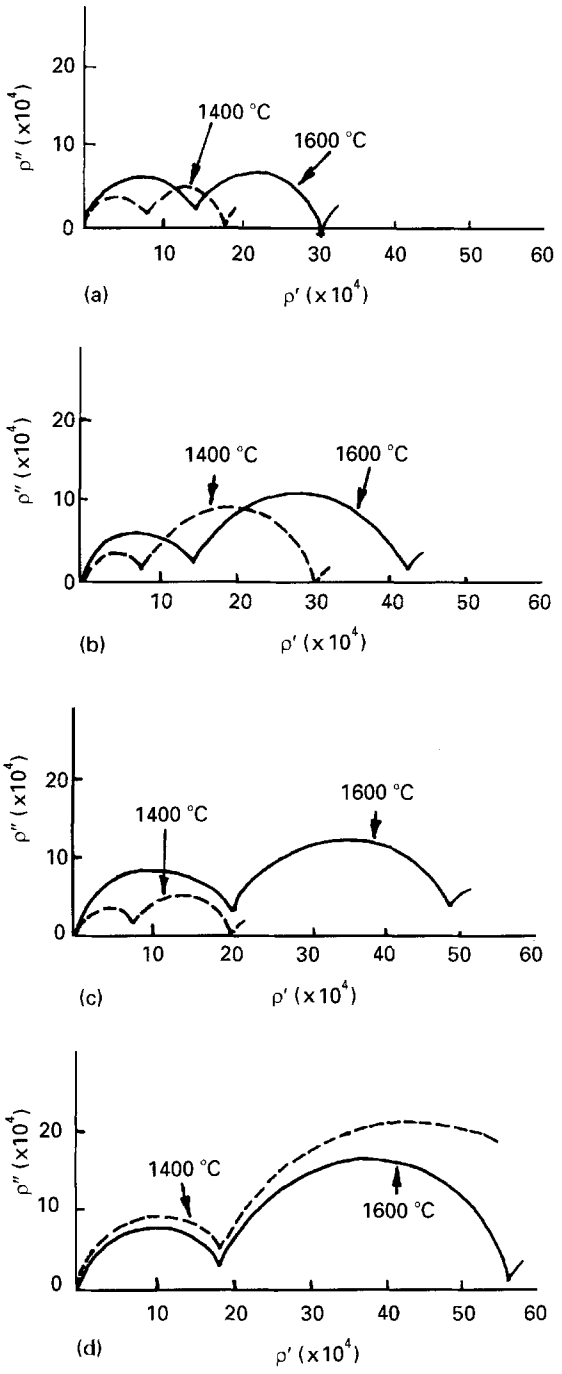

Figure 10 Influence of Al_2O_3 content and sintering temperature on the a.c. resistivity of tetragonal zirconia at 300 °C. (a) Z-3Y; (b) Z-3Y/5A; (c) Z-3Y/10A; (d) Z-3Y/20A.

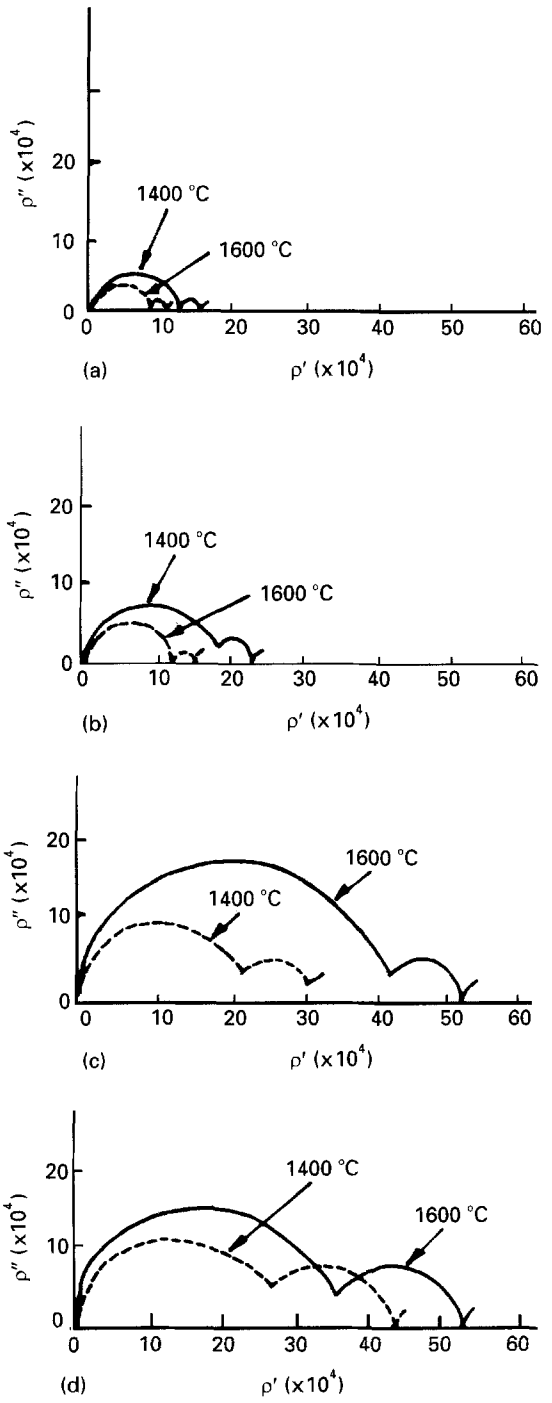

Figure 11 Influence of Al_2O_3 content and sintering temperature on the a.c. resistivity of cubic zirconia at 300 °C. (a) Z-8Y; (b) Z-8Y/5A; (c) Z-8Y/10A; (d) Z-8Y/20A.

Al_2O_3 to cubic zirconia could explain the improvement of the bending strength, cubic zirconia exhibits a certain plasticity at high temperature [29] and this contribution should also be taken into account. Bending strength values as high as 250 MPa were measured at 1000 °C, which is very near to the value at room temperature (300 MPa).

As reported in Fig. 6, the fresh fracture morphology of the cubic zirconia/Al_2O_3 composites after the bending strength test at 1000 °C underwent a transition from transgranular, for cubic zirconia without Al_2O_3, to intergranular for cubic zirconia containing 10 and 20 wt % Al_2O_3. According to the suggestions of French *et al.* [30], a higher intergranular fracture mode was present in the tougher Al_2O_3–c–ZrO_2 composites. This means that Al_2O_3 additions, inhibiting the grain growth of cubic zirconia, led to the formation of a microstructure with a higher grain boundary density and, therefore, a larger possibility of crack deflection. If, as reported by Bouma *et al.* [31], every deflection consumes energy, then a higher grain boundary density will lead to a higher energy use and, thus, to a higher fracture strength. Al_2O_3 additions decreased the cubic zirconia grain size from ~ 24 μm without Al_2O_3 to 4 μm and 3 μm for zirconia containing 10 and 20 wt % Al_2O_3, respectively [2].

The electrical conductivity of the yttria-doped zirconia/Al_2O_3 composites is the most important requirement to elucidate its usefulness as an electrolyte

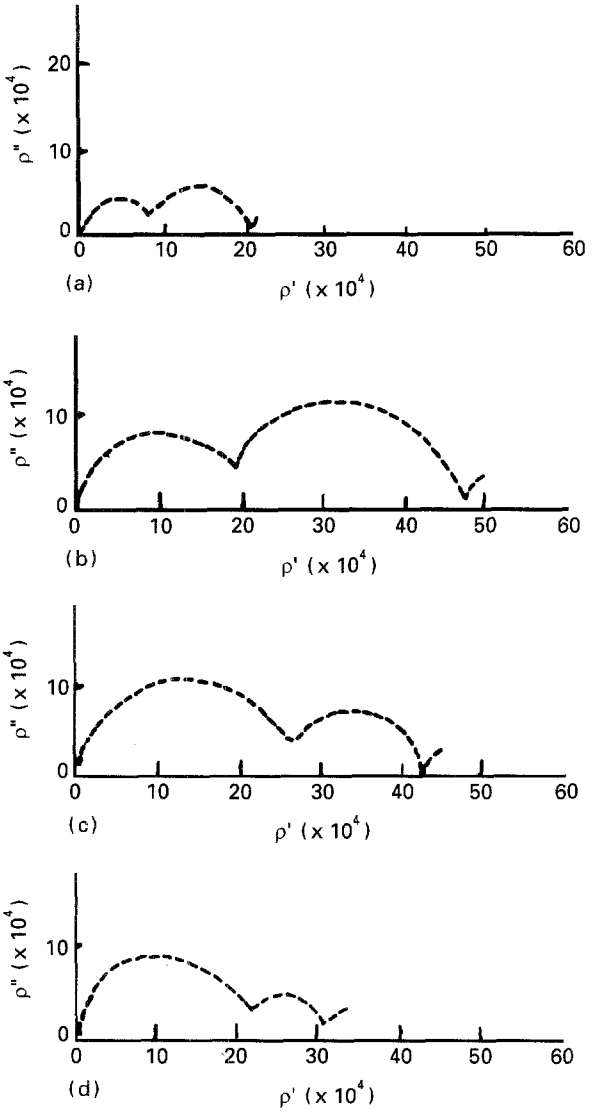

Figure 12 Effect of 10 wt % Al_2O_3 on the a.c. resistivity of different commercial yttria-doped zirconia samples at 300 °C. (a) Z-3Y/10A; (b) Z-4Y/10A; (c) Z-6Y/10A; (d) Z-8Y/10A.

in SOFC systems. As shown in Fig. 10 for tetragonal zirconia/Al_2O_3 composites, two clear arcs were observed in the complex plane impedance diagram recorded at 300 °C. The smaller one is due to the lattice oxygen ion conduction and remained constant up to a 10 wt % Al_2O_3 content. For higher Al_2O_3 content, the size of this first arc increased. The second arc, due to the grain boundary contribution to the total resistivity of the sample, increased its size with Al_2O_3 content, passing apparently through a minimum at 10 wt %. It has been shown elsewhere [2] that the grain size of the tetragonal zirconia samples hardly varied with Al_2O_3 content and, therefore, the decrease in resistivity up to 10 wt % could be attributed to a decrease in the grain boundary density. The increase in resistivity above 10 wt % Al_2O_3 could be due to both the coalescence of Al_2O_3 particles and the decrease in the volume fraction of the conducting phase in the sample. Rajendran *et al.* [19] published similar results on a 2.5 mol % Y_2O_3 tetragonal zirconia sintered at 1700 °C. At this sintering temperature a two-phase (tetragonal + cubic) was present in his sample, according to the the ZrO_2–Y_2O_3 phase diagram [22] and, as a consequence of this, an overlappping of the lattice and grain boundary arcs was present. In this way a decrease in the grain boundary density and a decrease in the resistivity per unit surface area was also found. The improvement in total conductivity was attributed to an accumulation of the grain-boundary glassy phase at the tetragonal zirconia/Al_2O_3 interfaces from the tetragonal/tetragonal ones [32]. The non-appearance of silica in our energy dispersive X-ray analyses on the sintered zirconia samples makes one think that another phenomenon could be contributing to the apparent improvement in conductivity.

As shown in Fig. 12, the influence of 10 wt % Al_2O_3 addition on zirconia containing different Y_2O_3 concentrations is a consequence of the amounts of the

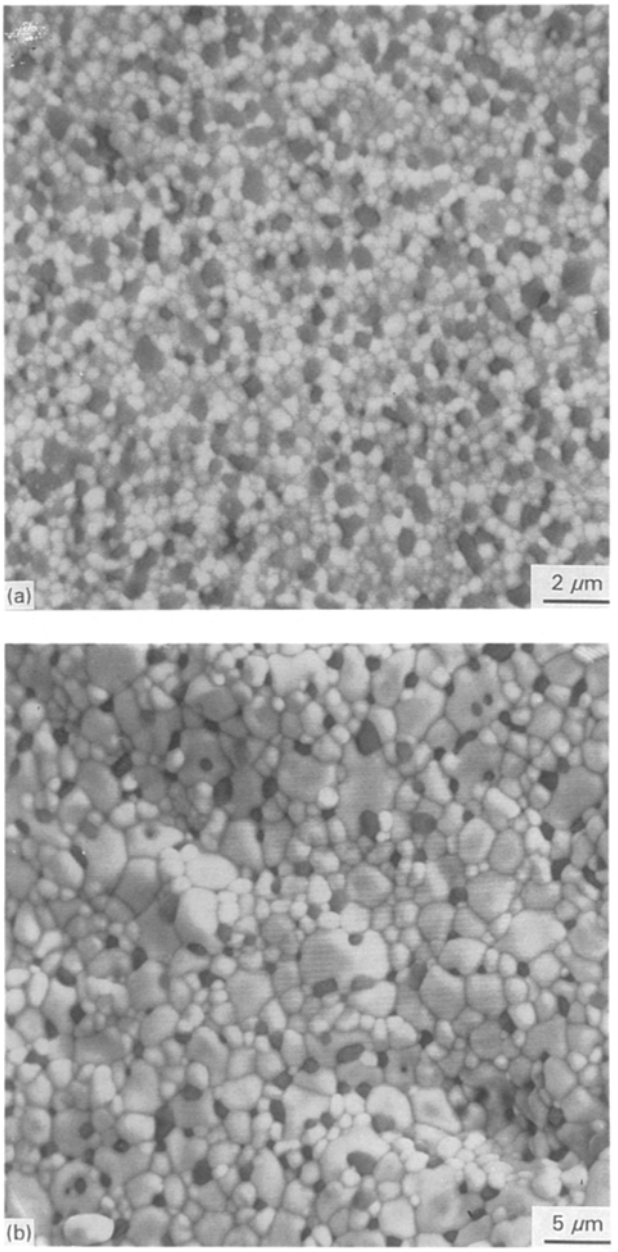

Figure 13 Microstructure of sintered yttria-doped zirconia/Al_2O_3 commercial composites. (a) Z-3Y/10A, (b) Z-4Y/10A, (c) Z-6Y/10A and (d) Z-8Y/10A.

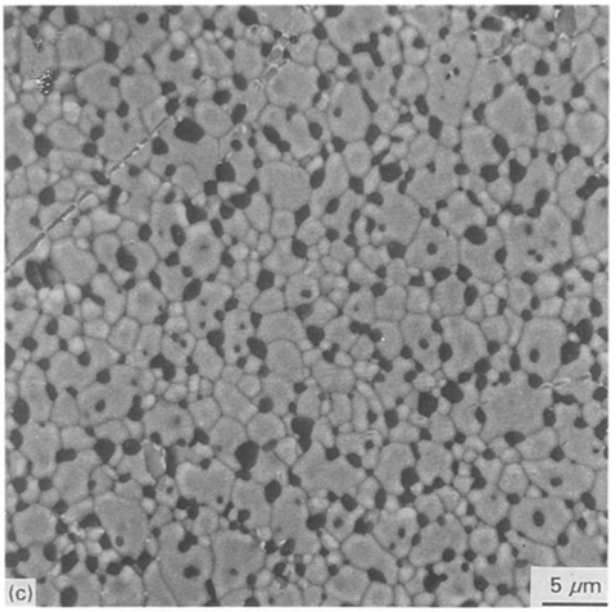

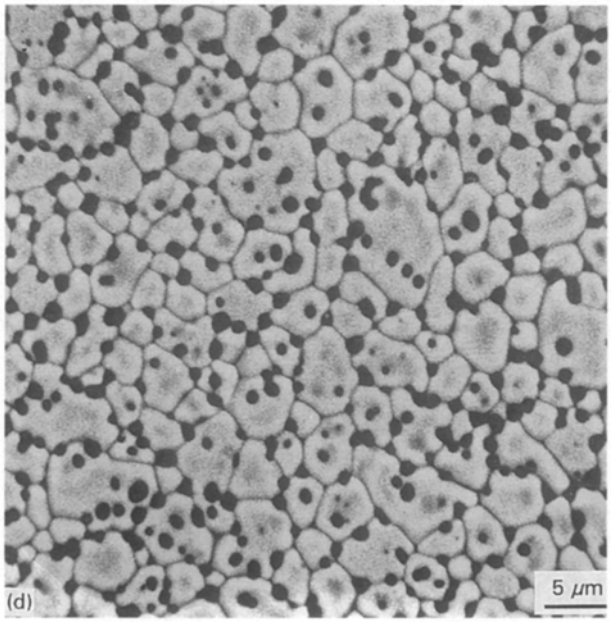

Figure 13 Continued.

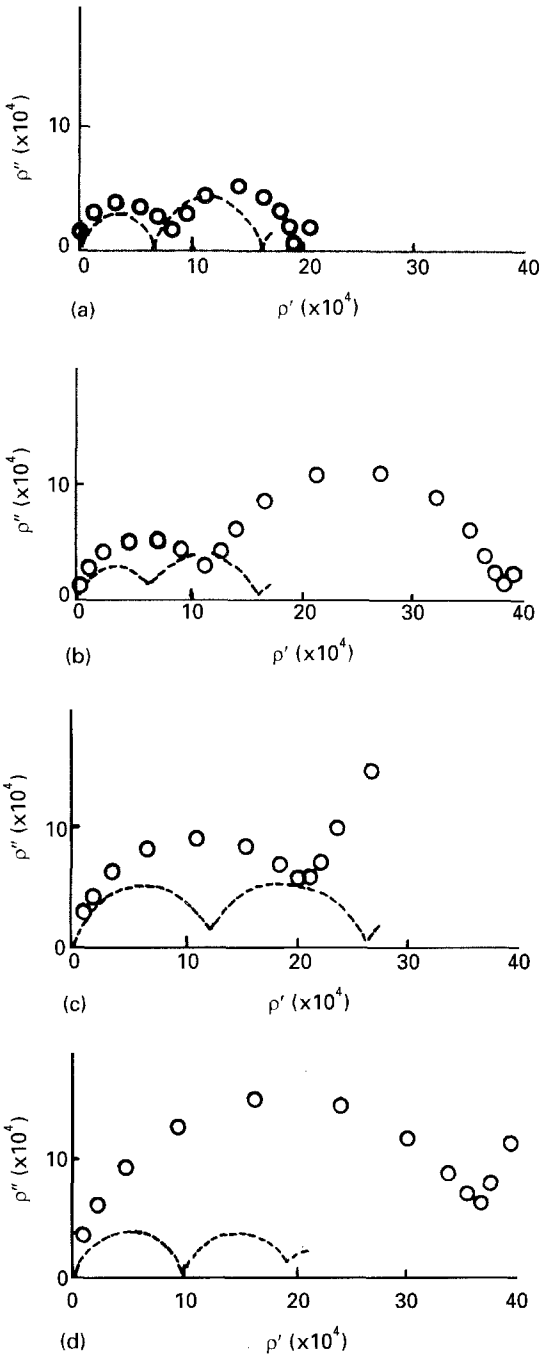

Figure 15 Typical impedance plots (measured at 300 °C) for different coprecipitated yttria-doped zirconia samples without and with 10 wt % Al_2O_3. (a) – – – Z-3Y, ○○○ Z-3Y/10A; (b) – – – Z-4Y, ○○○ Z-4Y/10A; (c) – – – Z-6Y, ○○○ Z-6Y/10A; (d) – – – Z-8Y, ○○○ Z-8Y/10A.

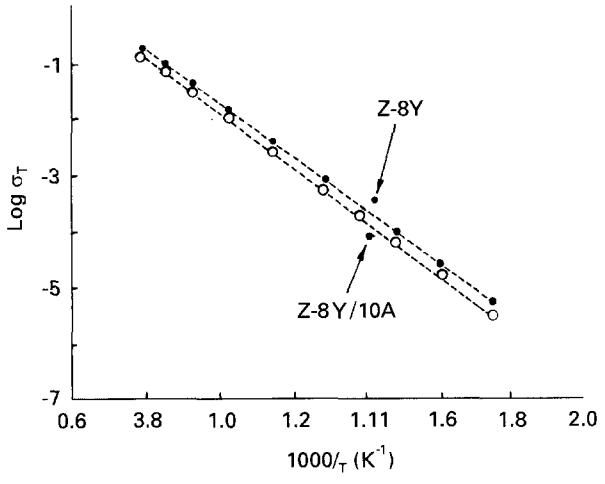

Figure 14 Temperature dependence of total conductivity σ_T of commercial cubic zirconia and cubic zirconia/10 wt % Al_2O_3 composite.

coexisting tetragonal and cubic phases in the sintered samples, and it is difficult to correlate the microstructure with the electrical behaviour. However, it is clear that the Al_2O_3 additions have a greater effect on those samples that have a single zirconia phase. Except in the case of the tetragonal zirconia, an addition of 10 wt % Al_2O_3 decreased the total conductivity of the sintered zirconia samples. The increase in the size of the two arcs, mainly the grain boundary one, shows evidence of this fact.

Concerning the cubic stabilized zirconia/Al_2O_3 composites (Z-8Y/Al_2O_3), it has been shown elsewhere [2] that Al_2O_3 additions decreased the zirconia

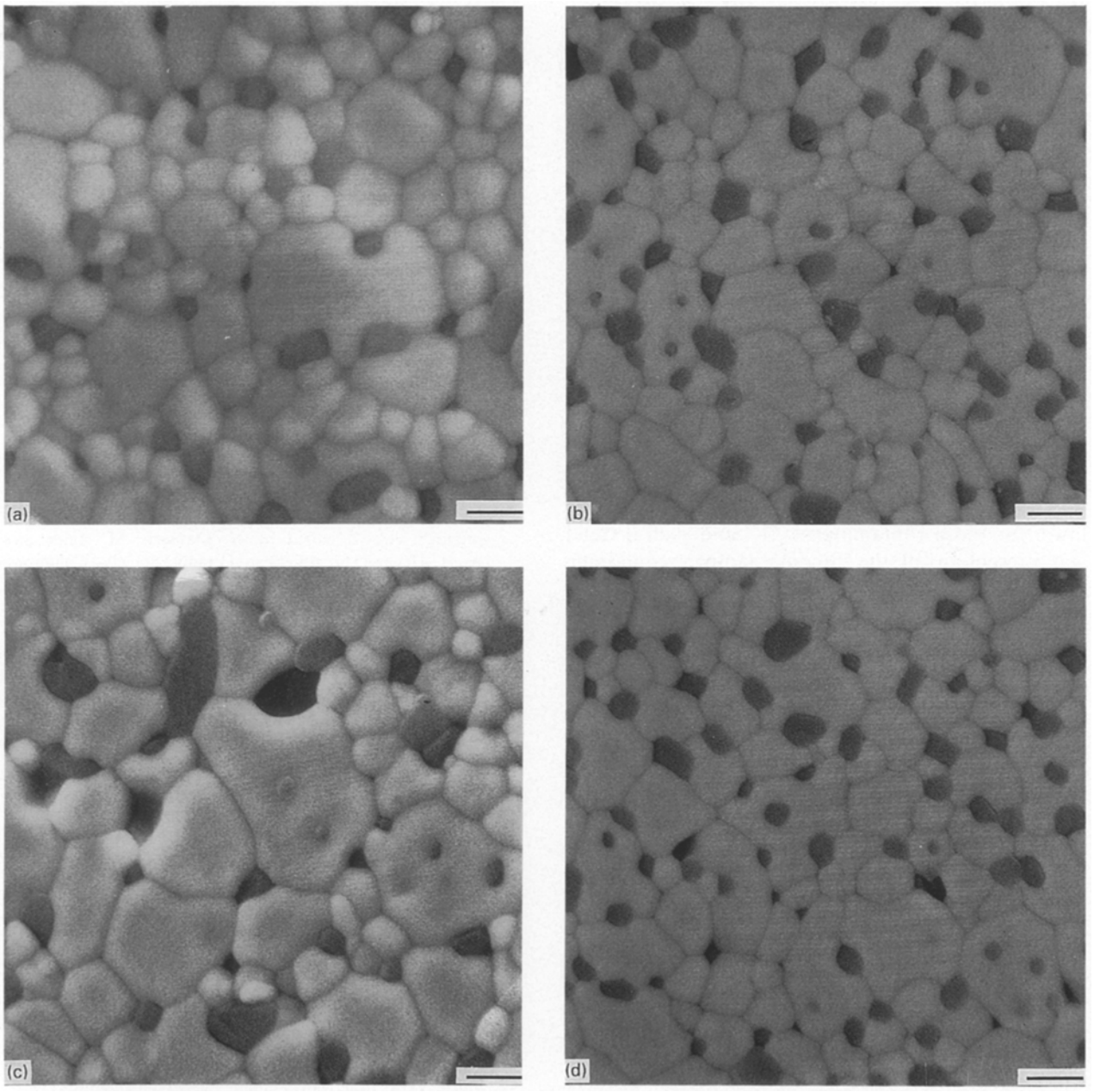

Figure 16 Scanning electron micrographs of commercial (a) Z-4Y/10A and (b) Z-6Y/10A samples, and coprecipitated (c) Z-4Y/10A and (d) Z-6Y/10A samples.

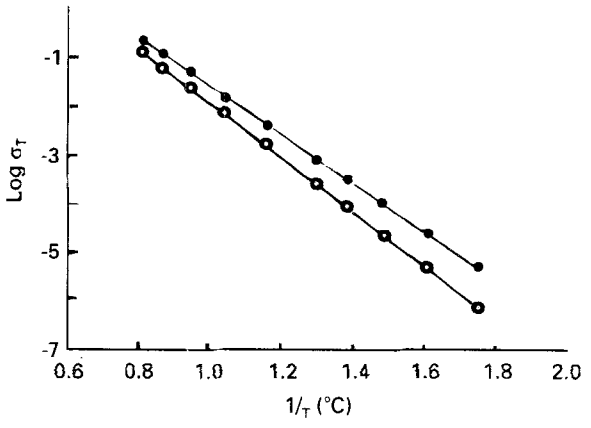

Figure 17 Arrhenius plots of the electrical conductivity σ_T for co-precipitated Z-8Y and Z-8Y/10A composite samples. ●—● Z-8Y; ○—○ Z-8Y/10A.

grain size from 25 μm without Al_2O_3 to 3 μm with 20 wt % Al_2O_3 at 1600 °C and from 3.5 μm to 2 μm at 1400 °C. Fig. 11 shows the resistivity in the complex plane impedance diagrams measured at 300 °C for Z-8Y samples with different alumina content (0–20 wt % Al_2O_3). Two well-defined arcs were observed up to 5 wt % Al_2O_3, and two overlapping arcs were observed in the Z-8Y containing 10 and 20 wt % Al_2O_3. As can be seen, the size of the lattice resistance arc (on the left-hand side) is strongly dependent on both the Al_2O_3 content and the sintering temperature, and such a correlation was more clearly evinced at the higher (1600 °C) sintering temperature. For this sintering temperature the size of the lattice arc increased with increasing Al_2O_3 content up to 10 wt % and then decreased. At the lower (1400 °C) sintering temperature the size of the lattice arc increased with

increasing Al_2O_3 content. The grain boundary arc (on the right-hand side) increased its size with increasing Al_2O_3 content, and such an increase was higher at the higher sintering temperature as a consequence of a higher zirconia grain growth inhibitor effect of Al_2O_3. No minima were detected either for lattice resistivity or for grain boundary resistivity as reported by Yamana *et al.* [33] at 5 wt % Al_2O_3 for a 5.5 mol % Y_2O_3 or by Miyayama *et al.* [23] for Al_2O_3 content higher than 0.6 mol %. Similarly, Yamamoto *et al.* [27] found better conductivities in fully stabilized zirconia with Al_2O_3 content up to 1 wt % and lower for higher Al_2O_3 content.

The Arrhenius behaviour of Z-8Y samples with and without Al_2O_3 additions, as shown in Fig. 14, is correlated to both the grain boundary and the lattice contributions to the total conductivity of the zirconia samples. A higher grain boundary conductivity was found in the samples without Al_2O_3 addition and lower for those containing Al_2O_3, and such a trend was present in all the zirconia samples containing different concentrations of Y_2O_3 and/or Al_2O_3 [34]. As reported by Yamana *et al.* [33], the grain boundary conductivities are closely related to the geometrical factors of the samples and these are strongly influenced by the grain size. Thus those zirconia samples with a high grain size (as for example Z-6Y and Z-8Y) will show a higher grain boundary conductivity, and the Arrhenius behaviour will be dominated by the lattice conductivity. Depending on the extent to which the Al_2O_3 additions influence not only the zirconia grain size but the zirconia–zirconia grain boundaries, assuming no other factors, the total conductivity of the zirconia sample will be enhanced.

An example of the above assumption was shown in Fig. 15 for the yttria-doped zirconia/Al_2O_3 co-precipitated samples, in which both the grain boundary and the lattice resistivities were strongly modified by the Al_2O_3 additions and yet their conductivities were higher than those of the commercial zirconia samples. Then other factors such as (a) the microstructure homogeneity, (b) the impurity level and its distribution, (c) the presence of a glassy phase, if any, and defects concentration of same and, finally, (d) the Al_2O_3 particles size and distribution in the zirconia matrix, should be taken into account to reach a satisfactory explanation for the yttria-doped zirconia/Al_2O_3 composites' electrical behaviour. The discrepancies found for the obtained results by different authors on similar, identical in some cases, zirconia samples, with and without Al_2O_3, support the above contention.

Acknowledgement

The authors thank Dr C. Baudín for many useful discussions and the JOULE Program for financing this work.

References

1. L. M. NAVARRO, P. RECIO and P. DURAN, *J. Mater. Sci.* This issue.
2. *Idem, ibid.* This issue.
3. B. C. H. STEELE, *Sci. Ceram.* **12** (1984) 697.
4. J. N. MICHAELS, C. G. VAYENAS and L. L. HEGEDUS, *J. Electrochem. Soc.* **133** (1986) 522.
5. D. C. FEE, R. K. STEUNENBERG, T. D. CLAAR, R. B. POEPPEL and J. P. ACKERMAN, Fuel Cell Seminar Abstract, (1983) 74.
6. S. IKEDA, O. SAKURAI, K. UEMATSU, N. MIZUTANI and M. KATOS, *J. Mater. Sci.* **20** (1985) 4593.
7. C. C. McPHEETERS and T. D. CLAARS, Fuel Cell Seminar Abstract, (1984) 64.
8. N. Q. MINH, in "Science and technology of zirconia", V., edited by S. P. S. Badwal, M. J. Bannister and R: H. J. Hannink (Technomic Publish Co. Inc., Switzerland, 1993) p. 652.
9. F. F. LANGE, *J. Mater. Sci.* **17** (1982) 247.
10. K. TSUKUMA and M. SHI'ADA, *J. Mater. Sci. Lett.* **4** (1985) 857.
11. T. SATO and M. SHIMADA, *J. Am. Ceram. Soc.* **68** (1985) 356.
12. *Idem, J. Mater. Sci.* **20** (1985) 3988.
13. E. P. BUTLER and J. DRENNAN, *J. Am. Ceram. Soc.* **65** (1982) 474.
14. H. BERBARD, Rep. LEA-R-5090, Commisariat à l'atomique, CEN-Saclay, France, 1981.
15. E. P. BUTLER, R. K. SLOTWINSKI, N. BONANOS, J. DRENNAN and B. C. H. STEELE, in "Advances in ceramics", Vol. 12, edited by N. Claussen, M. Ruhle and A. H. Heuer (The American Ceramic Society, Columbus, Ohio, 1984) p. 572.
16. M. V. INOZEMTSEV, M. V. PERFILEV and A. S. LIPILIN, *Elektrokhimiya* **10** (1974) 1471.
17. M. J. VERKERK, A. J. A. WINNUBST and A. J. BURGGRAAF, *J. Mater. Sci.* **17** (1982) 3113.
18. S. P. S. BADWAL, W. G. GARRET and M. J. BANNISTER, *J. Phys. E. Sci. Instrum*, in press.
19. S. RAJENDRAN, J. DRENNAN and S. P. S. BADWAL, *J. Mater. Sci. Lett.* **6** (1987) 1431.
20. G. R. ANSTIS, P. CHANTIKUL, B. R. LAWN and D. B. MARSHALL, *J. Am. Ceram. Soc.* **64** (1981) 533.
21. M. I. MENDELSOHN, *J. Am. Ceram. Soc.* **52** (1969) 443.
22. C. PASCUAL and P. DURAN, *J. Am. Ceram. Soc.* **66** (1983) 23.
23. M. MIYAYAMA, H. YANAGIDA and A. ASADA, *J. Am. Ceram. Soc.* **64** (1985) 660.
24. W. D. TUOIG and T. Y. TIEN, *J. Am. Ceram. Soc.* **63** (1980) 595.
25. A. KULCZYCKI and M. WASIUCIONEK, *Ceram. Inter.* **12** (1986) 181.
26. F. J. ESPER, K. H. FRIESE and H. GEIER, in "Advances in ceramics", Vol. 12, edited by N. Claussen, M. Ruhle and A. H. Heuer (The American Ceramic Society, Columbus, Ohio, 1984) p. 528.
27. O. YAMAMOTO, Y. TAKEDA, N. INAMISHI, T. KAWAHARA, G. Q. SHEN, M. MORI and T. ABE, in "Proceedings of the 2nd international symposium on solid oxide fuel cell", edited by P. Zegers *et al.*. European addendum, 1991, p.437.
28. S. RAJENDRAN, M. V. SWAIN and H. J. ROSSELL, *J. Mater. Sci.* **23** (1988) 1805.
29. K. MATSUSUE, Y. FUJISAWA and K. TAKUHARA, *Yogyo-Kyokai-Shi* **91** (1983) 59.
30. J. D. FRENCH, M. P. HARMER, H. M. CHAN and G. A. MILLER, *J. Am. Ceram. Soc.* **75** (1992) 418.
31. J. S. BOUMA, G. S. A. M. THEUNISSEN, A. J. A. WINNUBST and A. J. BURGGRAAF, in "Ceramics today–tomorrow's ceramics", edited by P. Vinzencini (Elsevier Science Publishing B. V., Amsterdam, 1991) p.1601.
32. J. DRENNAN and S. P. BADWAL, in "Advances in ceramics", vol. 24, edited by S. Samiya, N. Yamamoto and H. Yamagida (The American Ceramic Society, Columbus, Ohio, 1988) p.807.
33. K. YAMANA, S. NAKAMURA, T. YOSHIMURA and K. INA, *Solid State Ionics* **53–56** (1992) 763.
34. L. M. NAVARRO, Ph. D. Thesis, Alcalá de Henares University, Madrid, 1994.

Received 29 July 1994
and accepted 11 August 1994